

**Stem Cell Reports, Volume 12**

**Supplemental Information**

**Chemical Conversion of Human Fetal Astrocytes into Neurons through  
Modulation of Multiple Signaling Pathways**

**Jiu-Chao Yin, Lei Zhang, Ning-Xin Ma, Yue Wang, Grace Lee, Xiao-Yi Hou, Zhuo-Fan  
Lei, Feng-Yu Zhang, Feng-Ping Dong, Gang-Yi Wu, and Gong Chen**

## Supplemental figures and legends:

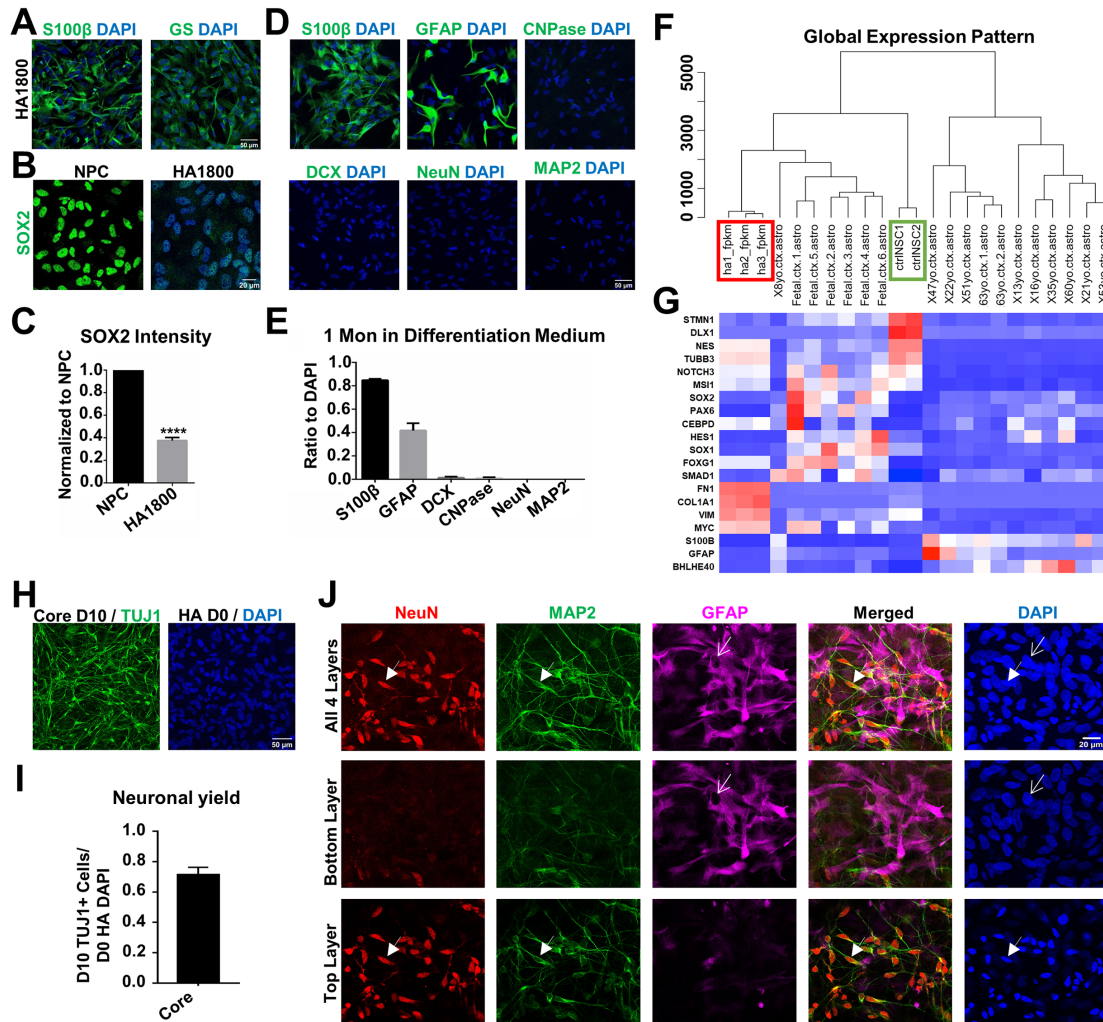


**Figure S1. Characterization of human cortical astrocytes, neuronal yield, and neuron-astrocyte co-cultures after conversion. Related to Figure 1.**

(A) Human astrocytes (HA1800, ScienCell) are immunopositive for astrocyte markers S100 $\beta$  and glutamine synthetase (GS).

(B-C) Human astrocytes are different from neuroprogenitor cells (NPCs). Immunostaining of stem cell marker SOX2 on NPCs and HA1800. Quantitative analysis showed much lower expression of SOX2 in human astrocytes than in NPCs. \*\*\*\* $p < 0.0001$ , unpaired  $t$  test. Data are represented in mean + SEM.  $N = 3$  batches.

(D-E) No neural differentiation in human astrocyte cultures. Human astrocytes were cultured in differentiation medium for 1 month, and then immunostained with astrocyte markers S100 $\beta$ , GFAP, new born neuron marker doublecortin (DCX), mature neuronal marker NeuN and MAP2, and oligodendrocyte marker CNPase (D). The number of each marker was quantified and the ratio to DAPI was calculated. After one month of culture,  $83 \pm 1\%$  of cells had S100 $\beta$  signal, while  $42 \pm 6\%$  were labelled by GFAP. Very few cells were found positive for neuronal markers or oligodendrocyte marker (E). Data are represented in mean + SEM.  $N = 3$  batches.

(F) Dendrogram of sample relationship based on global gene expression profiles. Our human astrocytes (red box) are more similar to human fetal astrocytes as reported before than human neural stem cell (green box) or human adult astrocytes. The datasets used for comparison are from previous studies (Modrek et al., 2017; Zhang et al., 2016b).

(G) Different expression profiles of some typical cell markers among human astrocytes and NSCs.

(H-I) Neuronal yield after core drug-induced neuron conversion. Immunostaining of neuronal marker TUJ1 was performed 10 days after initial drug treatment (H). Neuronal yield after core drug treatment (I,  $71.3 \pm 5.0\%$ ) was calculated as the number of TUJ1+ neurons divided by the number of initial human astrocytes (DAPI staining for cell count). N = 3 batches.

(J) Converted neurons and non-converted astrocytes form a nice co-culture system. 14 days after the initiation of drug treatment, we performed immunostaining with astrocyte marker GFAP (magenta) and neuronal markers NeuN (red) and MAP2 (green). Multiple layers of Z-stack images were taken using a Zeiss confocal microscope. The upper panel showed projected images of all four layers. Bottom layer showed mostly GFAP signals (open arrow) but few NeuN or MAP2 signal. Top layer showed mainly NeuN and MAP2 signal (solid arrow) but little GFAP signal, suggesting that neurons were on top of astrocytes after conversion. N = 3 batches.

Scale bars: A, D, H, 50  $\mu\text{m}$ ; B and J, 20  $\mu\text{m}$ .

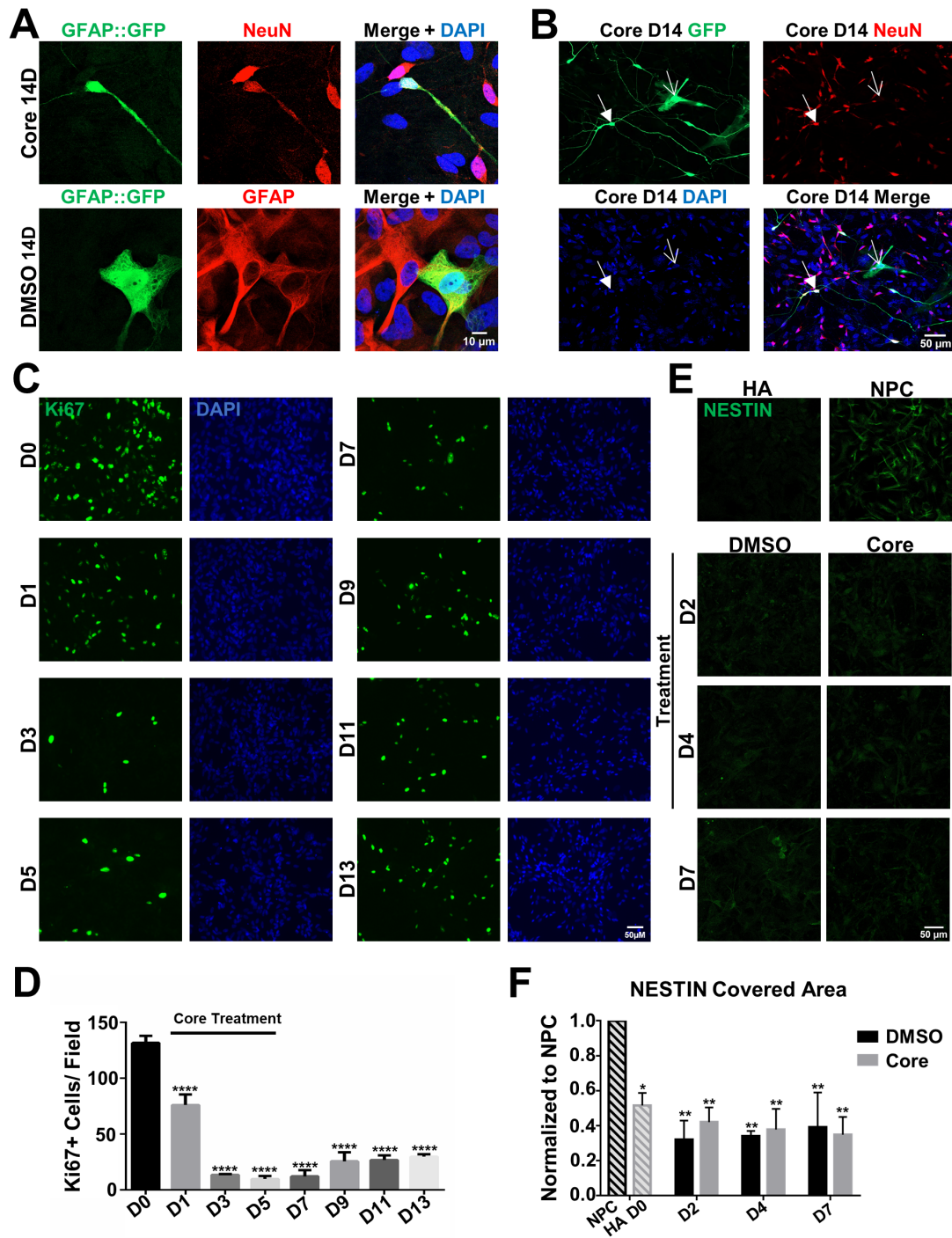


**Figure S2. Core drugs directly convert human astrocytes into neurons. Related to Figure 1.**

(A) Lineage tracing illustrates direct astrocyte-to-neuron conversion. Human astrocytes were infected with GFAP::GFP retrovirus for lineage tracing. Cells were then treated with either DMSO or Core drugs for 6 days. 14 days after initial drug treatment, immunostaining of GFP (Green), GFAP (Red) and NeuN (Red) were performed. In DMSO control group (Lower panel), GFP+ cells were GFAP+ astrocytes; while in core drug group (Upper panel), GFP+ cells were converted into NeuN+ neurons. N = 3 batches.

(B) Immunostaining after time-lapse imaging (see supplementary Movie S1) revealed that the majority of GFP-labeled cells with long processes were NeuN-positive neurons (labeled by solid arrow), while open arrow indicates a cell that stayed as astrocyte morphology. N = 3 batches.

(C-D) Assessment of cell proliferation after drug treatment. Human astrocytes were treated with core drugs from D1-D6. Immunostaining of cell proliferation marker Ki67 was performed before (D0), during (D1, D3, D5) and after (D7, D9, D11 and D13) drug treatment (C). Quantification of cell proliferation changes after core drug treatment. Ki67 positive cells were quantified in each 20x field. Cell proliferation rate significantly decreased during core drug treatment compared to D0 before drug application. A slight increase of cell proliferation was observed after drug removal (D). \*\*\*\* $p < 0.0001$ , One-way ANOVA, Dunnett's multiple comparisons test. Data are represented as mean + SEM. N = 3 batches.

(E-F) No progenitor cells generated during core drug treatment. DMSO and core drugs were applied to human astrocytes from D1 to D6. Neuroprogenitor cell marker NESTIN signal (E, Green) was monitored before, during (D2, D4), and after DMSO or core treatment (D7). Statistical analyses showed a significant difference of NESTIN signal between neuroprogenitor cells (NPC) and all human astrocyte groups, whether treated with DMSO or core drugs (F). Two-way ANOVA followed by Dunnett's multiple comparisons test. \* $p < 0.05$ , \*\* $p < 0.01$ . Data are represented in mean + SEM. N = 3 batches.

Scale bars: A, 10  $\mu\text{m}$ ; B, C, E, 50  $\mu\text{m}$ .

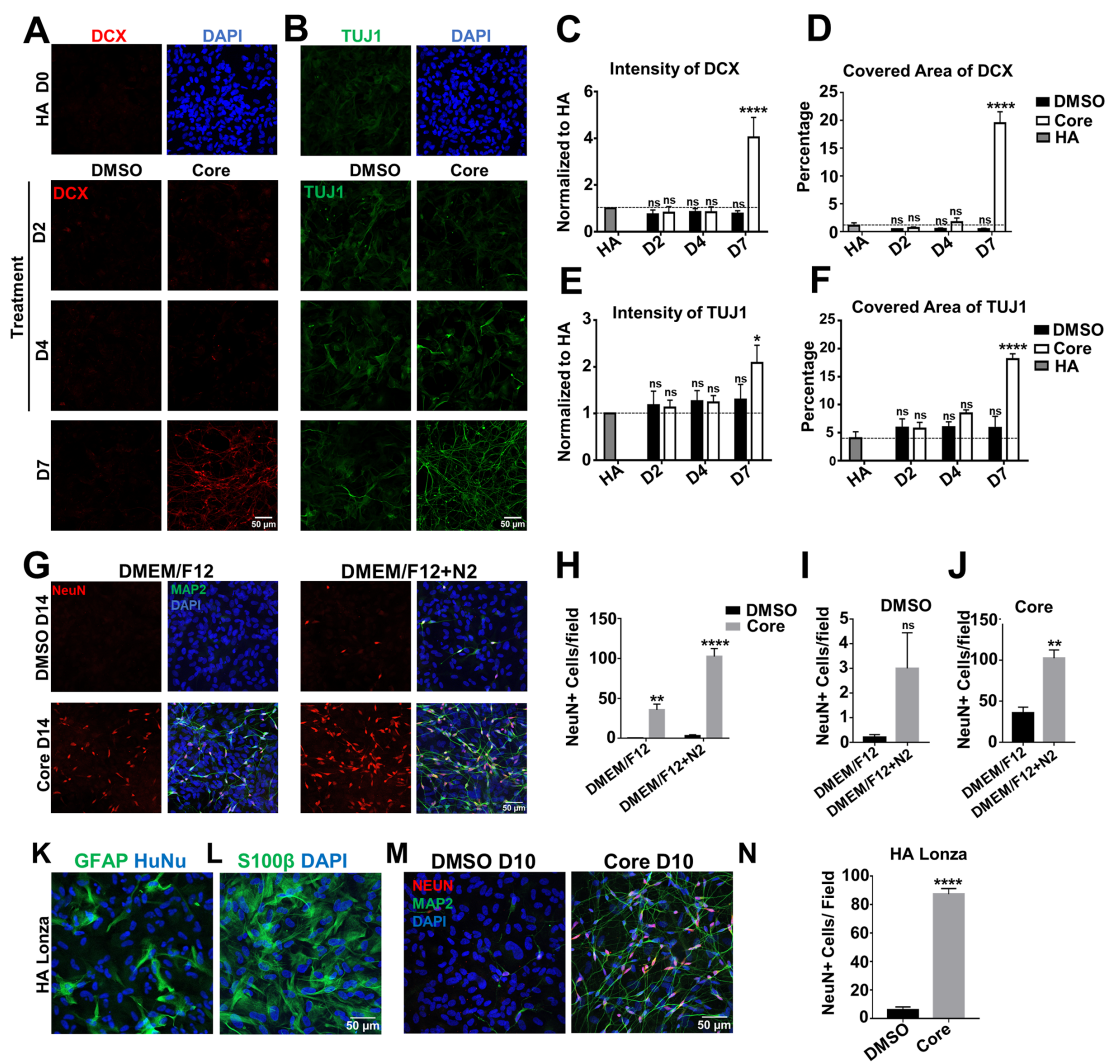


**Figure S3. Further characterization of early conversion process. Related to Figure 1.**

(A-F) Investigation of chemical conversion during early days using immature neuronal markers. DCX (A, red) and TUJ1 (B, green) immunostaining was performed before (D0), during (D2, D4) and after DMSO or core treatment (D7), to monitor newborn neurons (A-B). Statistical analyses of DCX signal (C-D) or TUJ1 signal (E-F) showed no change in DMSO control group, but a dramatic increase in core drug group at D7. Two-way ANOVA followed by Dunnett's multiple comparisons test. \* $p < 0.05$ , \*\*\*\* $p < 0.0001$ . Data are represented in mean + SEM.  $N = 3$  batches.

(G-J) N2 has a weak neural induction effect. DMSO or Core drugs were applied to human astrocytes in culture medium either with DMEM/F12 alone or DMEM/F12 + N2 supplement. Immunofluorescent staining of neuronal markers NeuN (G, red) and MAP2 (G, green) was performed at day 14. The number of NeuN+ cells was quantified in each field. In both medium, core drug group showed a large number of NeuN+ cells, which was significantly different from DMSO group (H). DMSO control group with DMEM/F12 alone produced almost no NeuN+ cells, while DMEM/F12 + N2 supplement showed ~3 NeuN+ cells in each field (I), suggesting a weak neural induction effect of N2 supplement. Core drugs in DMEM/F12 + N2 medium also induced more neurons from human astrocytes, compared to that in DMEM/F12 alone (J). Two-way ANOVA followed by Sidak's multiple comparisons test. \*\* $p < 0.01$ , \*\*\*\* $p < 0.0001$ . Data are represented in mean + SEM.  $N = 3$  batches.

(K-L) Human astrocytes purchased from Lonza were characterized by human nuclei marker HuNu (K, Blue), and astrocyte markers GFAP (K, Green) and S100 $\beta$  (L, Green).

(M-N) Chemical conversion of Lonza astrocytes into neurons after core drug treatment. Core drugs (2.5  $\mu$ M SB431542, 0.125  $\mu$ M LDN193189, 0.75  $\mu$ M CHIR99021 and 2.5  $\mu$ M DAPT) or 0.1% DMSO were added to Lonza astrocytes for 4 days, then replaced by neuronal differentiation medium.

Immunohistochemistry of neuronal markers NeuN (M, red) and MAP2 (M, green) was performed 10 days after initial drug treatment. Core drug group showed a large number of neurons compared to the control group (N). \*\*\*\* $p < 0.0001$ , unpaired  $t$  test. Data are represented in mean + SEM. N = 3 batches.

Scale bars: A, B, G, K, L, M, 50  $\mu$ m.

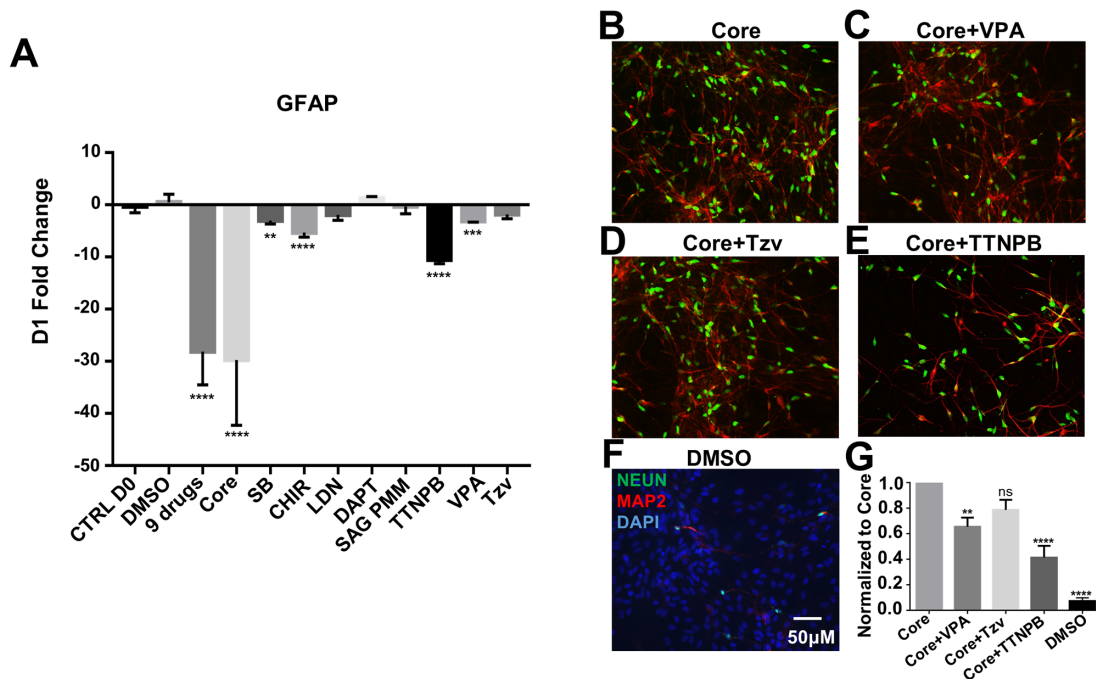


**Figure S4. Downregulation of glial genes by small molecules. Related to Figure 2.**

(A) Quantitative real-time PCR analyses showed a significant downregulation of GFAP in human astrocytes after 1-day core drug treatment. GFAP was dramatically downregulated by both 9 drugs and core drugs. Among individual drugs, SB431542, CHIR99021, TTNPB and VPA also significantly decreased GFAP. \*\* $p < 0.01$ , \*\*\* $p < 0.001$ , \*\*\*\* $p < 0.0001$ , One-way ANOVA after  $\log_2$  transformation, Dunnett's multiple comparison test. Data are represented in mean + SEM. N = 3 batches.

(B-F) Addition of extra drugs did not improve conversion efficiency. Human astrocytes were treated with core drugs (B), core drugs plus 0.1 mM VPA (C), or 0.5  $\mu$ M Tzv (D), or 0.5  $\mu$ M TTNPB (E) for 6 days. 0.2% DMSO (F) served as control group. Immunostaining of NeuN (green) and MAP2 (red) was performed at day 14 after the initiation of drug treatment. Scale bar: B-F, 50  $\mu$ m.

(G) Quantified data showing a decrease of conversion efficiency after addition of drugs to the core-drug formula. The number of NeuN-positive cells in each field was quantified, and each group was normalized to the core drug group. The addition of Tzv did not change the reprogramming efficiency, while VPA and TTNPB both decreased the reprogramming efficiency. \*\* $p < 0.01$ , \*\*\*\* $p < 0.0001$ , One-way ANOVA, Dunnett's multiple comparisons test. Data are represented in mean + SEM. N = 3 batches.



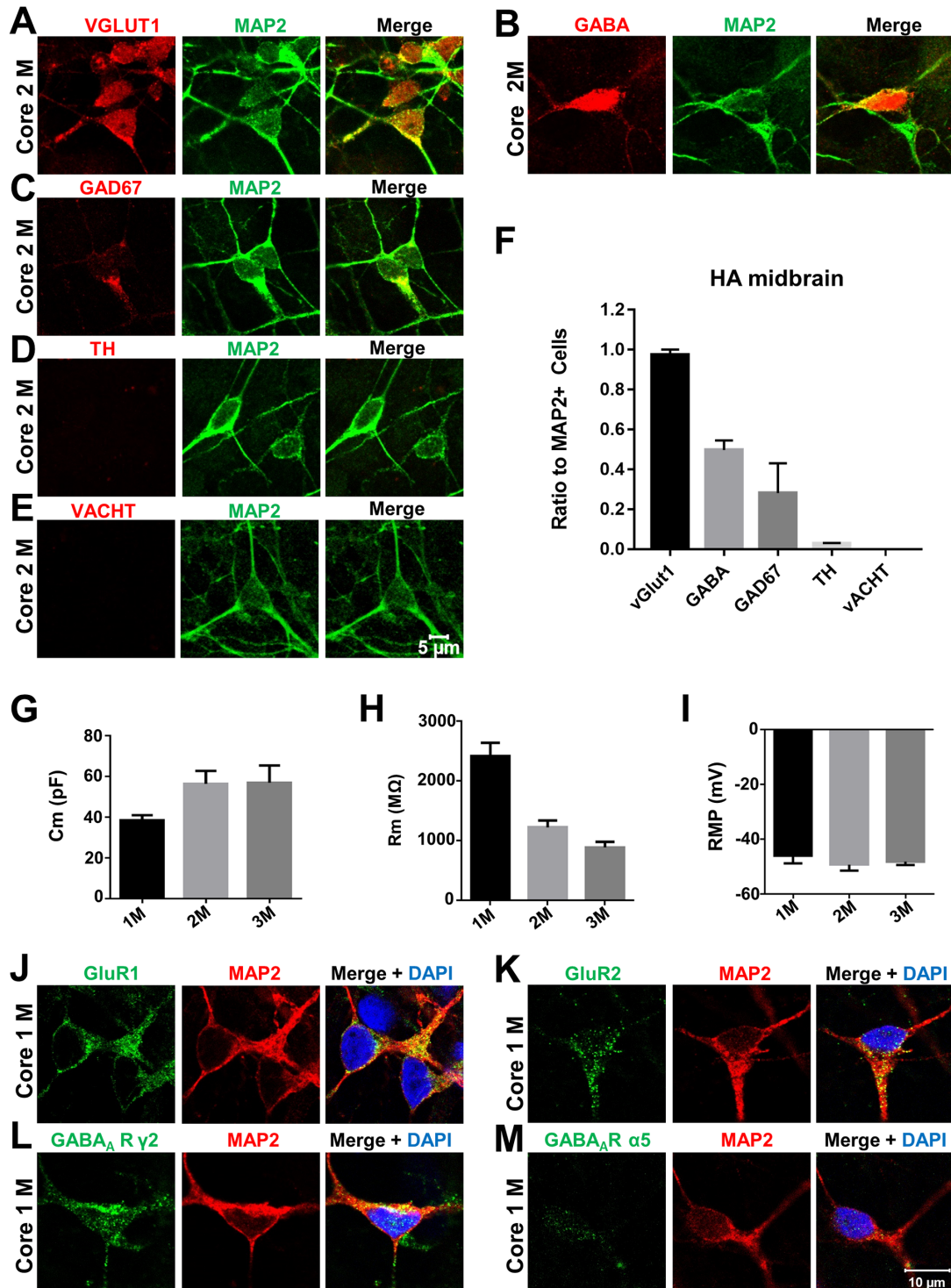


**Figure S5. Some GABAergic neurons are induced from human midbrain astrocytes by core drugs. Related to Figure 3 and Figure 4.**

(A-F) Core drug-induced chemical conversion in human midbrain astrocytes. Human midbrain astrocytes (ScienCell) were treated with core drugs for 6 days and then cultured for 2 months. Immunostaining of different neuronal subtype markers was performed. Human midbrain astrocyte-converted neurons (MAP2,

green) induced by core drugs were mainly glutamatergic (A, VGlut1, red,  $97.4 \pm 2.6\%$ ). Interestingly, some iNs also showed GABAergic neuron markers, such as GABA (B, red,  $49.8 \pm 4.7\%$ ) or GAD67 (C, red,  $28.1 \pm 15.0\%$ ), but dopaminergic (D, TH, Red,  $2.8 \pm 1.7\%$ ) or cholinergic neurons (E, VACHT, RED, 0%) were rarely detected. F, quantified data showing different subtypes of neurons after core drug treatment. Quantitative data were represented in mean + SEM (F). N = 3 batches.

(G-I) Developmental change of membrane capacitance (Cm, G), membrane resistance (Rm, H), and resting membrane potential (RMP, I) of core drug-induced neurons from 1 month to 3 months cultures. Data were represented by mean + SEM. N > 30 in each group.

(J-M) 1 month after core treatment, converted neurons (MAP2, red) expressed both glutamate receptors, shown by immunostaining of GluR1 (J, green) and GluR2 (K, green) subunits, and GABA<sub>A</sub> receptors shown by immunostaining of  $\gamma 2$  (L, green) and  $\alpha 5$  subunits (M, green). N = 3 batches.

Scale bars: A-E, 5  $\mu\text{m}$ ; J-M, 10  $\mu\text{m}$ .

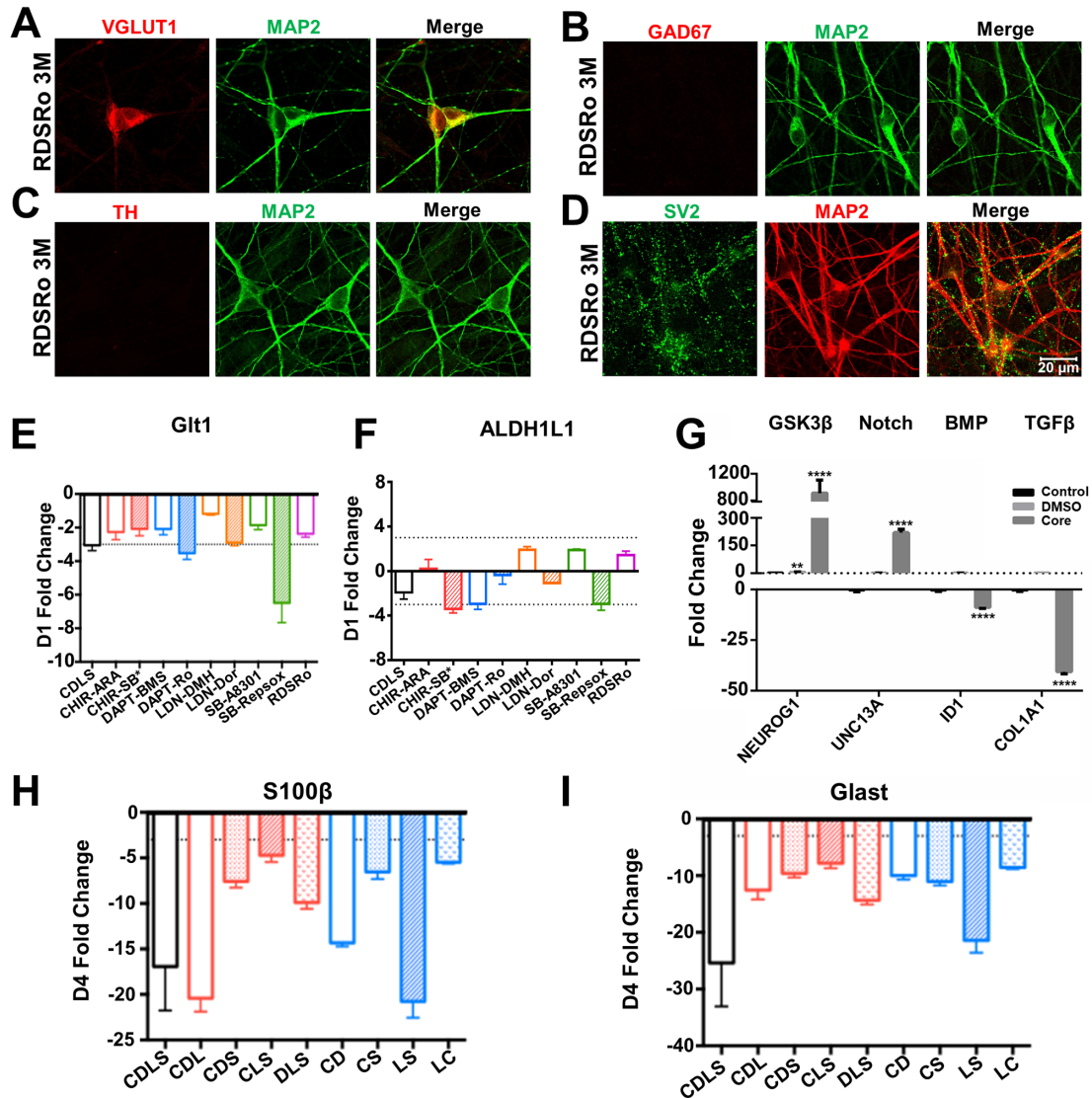


**Figure S6. Chemical conversion mediated by various combinations of small molecules. Related to Figure 5 and Figure 6.**

(A-C) The functional analogs of core drugs also converted human astrocytes (HA1800, ScienCell) into glutamatergic neurons. At 3 months after treatment with functional analogs including Repsox, Dorsomorphin, SB216763 and RO4929097 (RDSRo), most iNs showed vGlut1 signal (A, red), but not GAD67 (B, red) or TH signal (C, red). N = 3 batches.

(D) Three months after treatment with functional analogs (RDSRo), a large number of synaptic puncta (SV2, green) were found along MAP2-labelled dendrites (red). N = 3 bathes. Scale bar: A-D, 20  $\mu$ m.

(E-F) Downregulation of glial genes by functional analogs of core drugs. After 1-day treatment of core drugs or core drugs replaced by their functional analogues, real-time PCR analysis showed a decrease of astrocyte marker Glt1 (E) and mildly of ALDH1L1 (F). Dash line indicates 3-fold change. All data was normalized to D1 DMSO control group. Data are represented in mean + SEM. N = 3 batches.

(G) Signaling pathways affected by core drugs during reprogramming. Human astrocytes were treated with core drugs for 4 days, then collected for RT-PCR experiments. The expression of NEUROG1 is the direct

target of  $\beta$ -catenin in GSK3 $\beta$ -mediated pathway. UNC13A is the direct target of Notch pathway effector NICD. ID1 is the target gene of BMP pathway. COL1A1 is the target gene of TGF $\beta$  pathway. \*\* $p < 0.01$ , \*\*\* $p < 0.0001$ , One-way ANOVA after  $\log_2$  transformation, Dunnett's multiple comparisons test. Data are represented in mean + SEM. N = 3 batches.

(H-I) Downregulation of glial genes by 3 or 2 small molecules. Human astrocytes were treated with 4 core drugs (CDLS), 3-drug combinations (CDL, CDS, CLS, DLS) and 2-drug combinations (CD, CS, LS, LC). Real-time PCR analysis was performed on these drug combinations at D4 to analyze astrocytic markers S100 $\beta$  and Glast expression. All groups showed downregulation of S100 $\beta$  and Glast, compared to D0 human astrocytes. Dash line indicates 3-fold change. N = 3 batches.

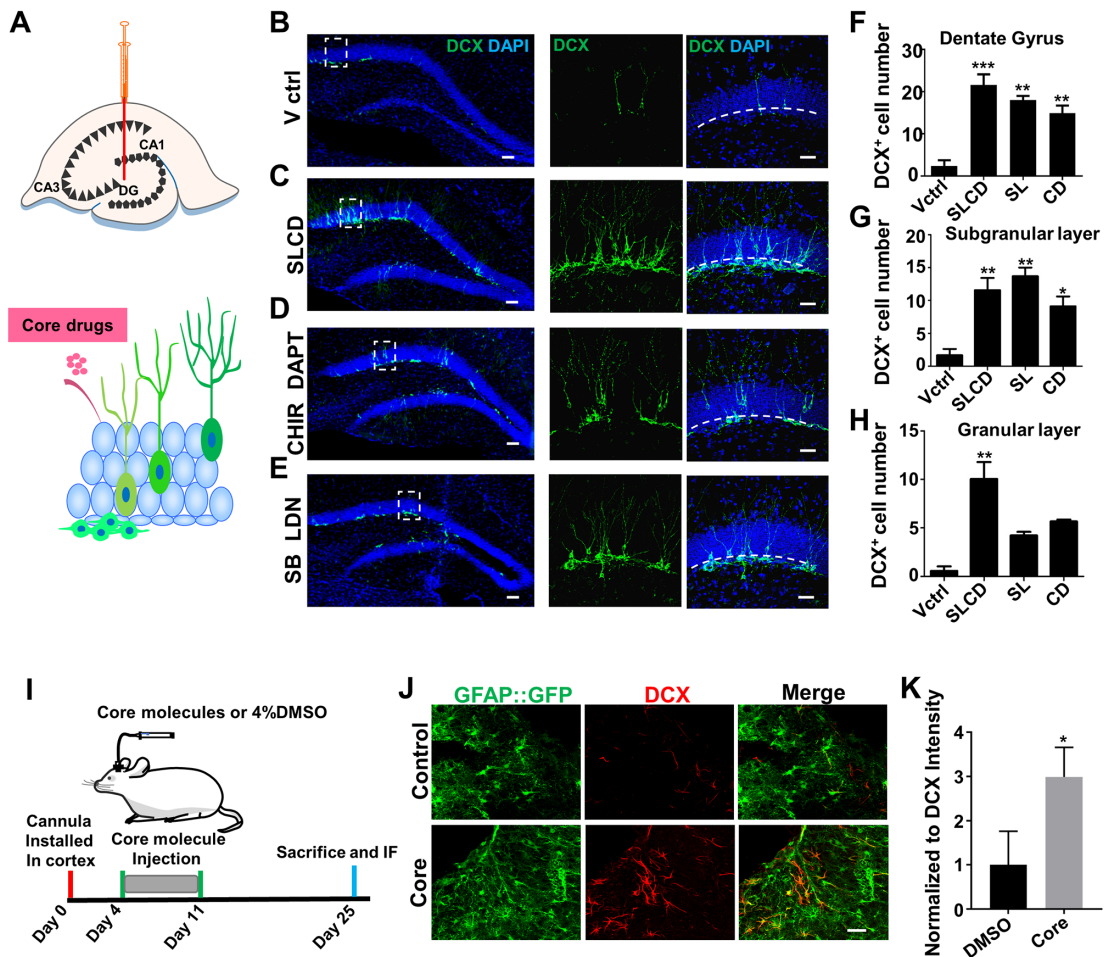


**Figure S7. Core drugs increased hippocampal neurogenesis and DCX+ cells in the cortex *in vivo*.** Related to Figure 7.

(A) Illustration of a single dose of drug injection into the dentate gyrus of mouse brains. After 7 days, the mice were sacrificed for immunostaining.

(B) When 4% DMSO was injected into the hippocampus of 1-year-old mouse, very few DCX+ newborn neurons were detected in the hippocampus.

(C-E) Injection of small molecules into the dentate gyrus with core drugs (C) (SB431542 50 $\mu$ M, LDN193189 5  $\mu$ M, CHIR99021 15  $\mu$ M, DAPT 50  $\mu$ M), or only two drugs of CHIR99021 + DAPT (D), or SB431542 + LDN99021 (E) significantly increased the DCX+ cell number in the subgranular layer (under the dash line) and granular layer (above dash line). Scale bars for B-E: left panel in low magnification, 60  $\mu$ m; right panels in high magnification, 30  $\mu$ m.

(F-H) Quantitative analysis revealed a significant increase of DCX+ cell number induced by small molecules in the entire dentate gyrus (F), or subgranular layer (G) and granular layer (H). \*  $P < 0.01$ , \*\*  $P < 0.001$ , \*\*\*  $P < 0.0001$ , one-way ANOVA followed by Dunnett's test.  $N = 3$  mice for each group.

(I) Schematic illustration of intracranial administration of small molecules through mini-osmotic pump. Brain cannula was installed in GFAP::GFP mouse cortex, where astrocytes were labeled green. Core drugs including SB431542 50  $\mu$ M, LDN193189 5  $\mu$ M, CHIR99021 15  $\mu$ M, and DAPT 50  $\mu$ M in a total volume of 100  $\mu$ l were perfused through mini-osmotic pump (Alzet, Cupertino, CA) for 7 days. In control mice, 4% DMSO was perfused as vehicle control. Mice received small molecules were sacrificed for

immunostaining 2 weeks after small molecule treatment.

(J-K) Representative images (J) and quantitative analysis (K) revealed an increased DCX expression in GFAP-expressing reactive astrocytes. No neuronal morphology was observed. N = 3 mice, Student t test \*  $P < 0.05$ , Scale bar for J, 30  $\mu\text{m}$ .

**Supplemental tables:**

**Table S1. Antibodies used for Immunostaining. Related to Figure 1-7 and Figure S1-S7.**

polyclonal anti-NEUN	rabbit, 1:1000, Millipore, ABN78
polyclonal anti-Microtubule Associated Protein 2 (MAP2)	chicken, 1:2000, Abcam, AB5392
monoclonal anti- $\beta$ III tubulin (TUJ1)	mouse, 1:1000, COVANCE, MMS-435P
polyclonal anti-MECP2	rabbit, 1: 500, Diagenode, 15410052
polyclonal anti-REST	rabbit, 1:600, Sigma, SAB2108706
polyclonal anti-T-box, brain, 1 (TBR1)	rabbit, 1: 300, Abcam, AB31940
polyclonal anti-PROX1	rabbit, 1:1000, ReliaTech GmbH, 102-PA32
monoclonal anti-CTIP2	rat, 1:600, Abcam, ab18465
anti-HOXB4	mouse, 1:200, Developmental Studies Hybridoma Bank, Iowa City, I12 anti Hoxb4
polyclonal anti-vesicular glutamate transporter 1 (VGLUT1)	rabbit, 1:1000, Synaptic Systems
monoclonal anti-GAD67	mouse, 1:1000 Millipore, MAB5406
monoclonal anti tyrosine hydroxylase (TH)	mouse, 1:600, Millipore, MAB318
polyclonal anti-vesicular glutamate transporter (SV2)	mouse, 1:1000, Developmental Studies Hybridoma Bank, Iowa City
polyclonal anti-green fluorescent protein (GFP)	chicken, 1:1000, Abcam, AB13970
polyclonal anti-glial fibrillary acidic protein (GFAP)	chicken, 1:1000, Millipore, AB5541
polyclonal anti-glial fibrillary acidic protein (GFAP)	Rabbit, 1:1000, Millipore, AB5804
monoclonal anti-Human Nuclei (HuNu)	mouse, 1:1000, Millipore, MAB1281
polyclonal anti-CDP (CUX1)	rabbit, 1:500, Santa Cruz, SC-13024
polyclonal anti-NURR1	rabbit, 1:2000, Santa Cruz, SC-991
monoclonal anti-S100 $\beta$	mouse, 1:800, Abcam, ab66028
monoclonal anti-Glutamine Synthetase (GS)	mouse, 1:800, Millipore, MAB302
monoclonal anti-CNPase	mouse, 1:800, Abcam, ab6319
polyclonal anti-Doublecortin (DCX)	rabbit, 1:500, Abcam, AB18723
polyclonal anti-Doublecortin (DCX)	goat, 1:500, Santa Cruz, sc-8066
polyclonal anti-SOX2	rabbit, 1:800, Millipore, AB5603
polyclonal anti-Ki67	rabbit, 1:800, Abcam, ab15580
Monoclonal anti-BrdU	rat, 1:1000, Accurate, OBT0030
Monoclonal anti-GluR1	mouse, 1:800, Millipore, MAB2263
Monoclonal anti-GluR2	mouse, 1:800, Millipore, MAB397
Polyclonal anti-GABA <sub>A</sub> receptor $\alpha$ 5 subunit	rabbit, 1:800, abcam, ab10098
Polyclonal anti-GABA <sub>A</sub> receptor $\gamma$ 2 subunit	Rabbit, 1:800, SYSY, 224003

**Table S2. Sequences of primers used in RT-PCR. Related to Figure 2, 3 & Figure S4, S6.**

<i>NGN2-F</i>	ATTTGCAATGGCTGGCATCT
<i>NGN2-R</i>	CACAGCCTGCAGACAGCAAT
<i>NEUROD1-F</i>	CCTGCAACTCAATCCTCGGA
<i>NEUROD1-R</i>	GGCATGTCCTGGTTCTGCTC
<i>GAPDH-F</i>	TGGGCTACACTGAGCACCAG
<i>GAPDH-R</i>	GGGTGTCGCTGTTGAAGTCA
<i>PROX1-F</i>	GCCAAACTCCTTACAACCGGA
<i>PROX1-R</i>	GGCCGAAAAGACTTTGACCAC
<i>CTIP2-F</i>	ACCTGTGGCCAGTGTCAAATG
<i>CTIP2-R</i>	TTGTCATAGCAGGCACCCAAG
<i>TBR1-F</i>	TGGATGTGATTTTGGCGGA
<i>TBR1-R</i>	CCGGATGCATATAGACCCGAT
<i>CUX1-F</i>	ATGCCACCGCAACGGTATT
<i>CUX1-R</i>	GCGCAAATCCTCTGGAGTGTT
<i>NURR1-F</i>	AATGCGTTTCGTGGCTTTGG
<i>NURR1-R</i>	AGCAATGCAGGAGAAGGCAGA
<i>HOXB4-F</i>	ACGGTAAACCCCAATTACGCC
<i>HOXB4-R</i>	TTTTCCACTTCATGCGCCG
<i>NEUN-F</i>	GCCCCGCTCGTTAAAAATG
<i>NEUN-R</i>	ACACGTCTCCAACATCCCCTT
<i>NEUROG1-F</i>	ACCGCATGCACAACCTTGAAC
<i>NEUROG1-R</i>	ATGTAGTTGTAGGCCAAGCGC
<i>UNC13A-F</i>	CTTTGTACAGACGCAATCGGC
<i>UNC13A-R</i>	TGTGTTCCCCAGTTCCTGGAT
<i>IDI-F</i>	CGTGCTGCTCTACGACATGAA
<i>IDI-R</i>	TGCTGGAGAATCTCCACCTTG
<i>COL1A1-F</i>	AATCACCTGCGTACAGAACGG
<i>COL1A1-R</i>	CAGATCACGTCATCGACAAC
<i>GFAP-F</i>	CGCAGTATGAGGCAATGGC
<i>GFAP-R</i>	ACCACTCTTCGGCTTCATGC
<i>Glt1-F</i>	CCAGGAAAAACCCCTTCTCCT
<i>Glt1-R</i>	CAACGAAAGGTGACAGGCAAA
<i>ALDH1L1-F</i>	CGCTGTACAACCGCTTCCTC
<i>ALDH1L1-R</i>	CCTGCACCATCCCTTTGATG
<i>S100<math>\beta</math>-F</i>	CCGAACTGAAGGAGCTCATCA
<i>S100<math>\beta</math>-R</i>	CATTCGCCGTCTCCATCATT
<i>Glast-F</i>	AGAACAATGGCGTGGACAAGC
<i>Glast-R</i>	AATGGCAGCCAAAGCCTCAT



## Supplemental Experimental Procedures:

### Time-lapse imaging

Human astrocytes were infected with CAG::GFP lentivirus in order to visualize the morphological change of astrocytes during and after drug treatment (Zhang et al., 2015). When the cells reached ~90% confluence, core drugs (5  $\mu$ M SB431542, 0.25  $\mu$ M LDN193189, 1.5  $\mu$ M CHIR99021 and 5  $\mu$ M DAPT) were added into N2 medium to reprogram human astrocytes, some of which were GFP-labeled after lentiviral infection. The cells were then put into the IncuCyte system (Essen BioScience, Ann Arbor, Michigan) for four continuous days without any medium change. Images were taken every two hours to trace the morphology change of human astrocytes. Drugs were withdrawn after four days and neuronal differentiation medium was added to the cells. Image taking was conducted until eight days, when most converted cells showed neuronal processes.

### Immunocytochemistry

Cells on coverslips were fixed in 4% PFA (Alfa Aesar) at room temperature for 12 min, and then PFA was washed off with PBS for three times. After washing, coverslips were transferred into blocking buffer, and incubated on the shaker in a slow speed for 1 hr. The blocking buffer was made of 2.5% normal donkey serum (Jackson ImmunoResearch), 2.5% normal goat serum (Jackson ImmunoResearch), 0.1% Triton X-100 (Fisher Scientific) in PBS. After blocking, cells were incubated in primary antibodies overnight at 4 °C. The second day, primary antibodies were washed off with PBS for three times. Then, cells were incubated in corresponding secondary antibodies for 1 hr in room temperature. Secondary antibodies were tagged with fluorophore Alexa Fluor 488, Alexa 594, Alexa 647 (1:800, Molecular Probes). After incubation, secondary antibodies were washed off with PBS for three times. Coverslips with cells were finally mounted on glass slides with mounting solution containing DAPI (Invitrogen). Triton was removed from blocking buffer for the staining of glutamate and GABA receptors. The immunostaining results were analyzed using fluorescent microscopes (Nikon ECLIPSE TE2000-S and ZEISS ApoTome). Confocal microscopes (Olympus FV1000 and ZEISS LSM800) were also used to take images. Antibodies were listed in Table S1.

### Electrophysiology

Multiclamp 700A patch-clamp amplifier (Molecular Devices, Palo Alto, CA) was used to perform whole-cell recordings. Coverslips with converted iNs were transferred into a recording chamber, which was constantly perfused with bath solution containing 128 mM NaCl, 30 mM glucose, 25 mM HEPES, 5 mM KCl, 2 mM Ca<sup>2+</sup>, and 1 mM MgCl<sub>2</sub>. The pH of bath solution was adjusted to 7.3 with NaOH, and osmolality was 300-305 mOsm/L. The pipette solution consisted of 135 mM KCl, 5 mM Na-phosphocreatine, 10 mM HEPES, 2 mM EGTA, 4 mM Mg-ATP, and 0.5 mM Na<sub>2</sub>GTP. The pH of pipette solution was adjusted to 7.3 with KOH, and osmolality to 280-290 mOsm/L. Patch pipettes were pulled from borosilicate glass, and the pipette resistance was 3-6 M $\Omega$  after filled with pipette solution. The series resistance after forming whole-cell recording was under 25 M $\Omega$  and not compensated during recording to reduce noise. For detecting spontaneous events and sodium and potassium currents, the membrane potential was held at -70 mV under voltage-clamp mode. Drug delivery was through a gravity-driven system (VC-6, Harvard Apparatus, Hamden, CT).

### RNA extraction

Human astrocytes were collected 1 day or 4 days after drug treatment. The 4-drug and 9-drug treatments were applied side-by-side. Macherey-Nagel NucleoSpin® RNA kit was used to isolate RNA from human astrocytes. 350  $\mu$ l lysis buffer and 3.5  $\mu$ l  $\beta$ -mercaptoethanol were added to each well of 24-well plate, and cell lysate was collected. After passing through one NucleoSpin® filter, RNA binds to the NucleoSpin® RNA column. After DNase treatment, and three times washing, RNA was purified. The pure RNA was eluted with 40  $\mu$ l RNase-free water, and RNA concentration was measured by NanoDrop. Isolated RNA was stored in -80 °C for reverse transcription.

## Reverse transcription and RT-PCR

Quanta Biosciences qScript<sup>TM</sup> cDNA SuperMix (5X) was used to synthesize cDNA from isolated RNA. 1 µg RNA template, 4 µl qScript<sup>TM</sup> cDNA SuperMix was used in each reaction. RNase/DNase-free water was added to make the reaction volume 20 µl. Then the reaction mix was incubated at 25 °C for 5 min, 42 °C for 30 min, and 85 °C for 5 min. cDNA was diluted in RNase/DNase free water for 5 times. Quanta Biosciences PerfeCTa<sup>TM</sup> SYBR® Green SuperMix, ROX<sup>TM</sup> was used for RT-PCR. 5 µl cDNA was used in 25 µl reaction volume. 40 PCR cycles, each of which contained 15 s at 95 °C and 45 s at 65 °C, were performed to amplify the reaction mix. Comparative Ct values were used to calculate the gene expression fold difference. GAPDH was used as the internal control, and relative Ct values were further normalized to human astrocytes collected at D0, before drug treatment. Each sample had three replicates in each PCR reaction. All RT-PCR data was log<sub>2</sub> transformed to fit normal distribution assumption of one-way ANOVA. Some primers were adapted from our recent 9-drug protocol (Zhang et al., 2015), and the sequences of all primers were listed in Table S2.

## RNA-sequencing Analysis

After RNA extraction, the qualities of human astrocyte samples were examined on Agilent 2100 bioanalyzer at UCLA Technology Center for Genomics & Bioinformatics, followed by mRNA enrichment and library construction. Single-end 50 bp sequencing was performed on HiSeq 3000. Quality check of the raw data was done using FastQC (v. 0.11.3), then reads were aligned against human reference genome hg38 using HISAT2 (v. 2.0.1) (Kim et al., 2015) and summarized using stringtie (v. 1.3.4) (Pertea et al., 2015). Genes with FPKM < 0.1 were removed. This RNAseq data is available in Gene Expression Omnibus (GEO: GSE123397). Datasets for induced neural stem cells (GSE94962) and human fetal & adult astrocytes (GSE73721) were published by previous studies (Modrek et al., 2017; Zhang et al., 2016).

## Lineage Tracing

Human astrocytes (ScienCell, 1800) cultured in 24-well plate were infected with 2 µl pGFAP::GFP-IRES-GFP retrovirus for overnight. Cells were then treated with 0.2% DMSO or small molecules. 14 days after treatment, cells were fixed for the immunostaining of neuronal markers and GFP.

## Stereotaxic injection of small molecules into mouse brain

All animal studies were approved by Penn State IACUC committee and in accordance with NIH guidelines on animal welfares. Brain surgeries were performed on 2-month old wild-type C57BL6 mice. Mice were anesthetized by injecting 20 mL/kg 0.25% Avertin (a mixture of 25 mg/ml of tribromoethylethanol and 25 µl/ml T-amyl-alcohol) into the peritoneum and then placed in a stereotaxic device. Artificial eye ointment was applied to cover and protect the eye. The animals were operated with a midline scalp incision and a drilling hole on the skull above somatosensory cortex. Each mouse received one injection in the dentate gyrus (coordinates: AP -2.06 mm, ML 1.5 mm, DV -2.1 mm) of small-molecule mixture [SB431542 (0.2 mM), LDN193189 (10 µM), CHIR99021 (60 µM) and DAPT (0.2 mM)] or PBS containing 2% DMSO with a 5 µl syringe and a 34 gauge needle. The injection volume and flow rate were controlled as 2 µl at 0.2 µl/min. After injection, the needle was kept for at least 5 additional minutes and then slowly withdrawn.

## Drug perfusion with mini-osmotic pump

Brain cannula was installed in GFAP::GFP mouse cortex, where astrocytes were labeled green (installation coordinate: AP 1.25 mm, ML 1.4 mm, DV -1 mm). Core drugs including SB431542 50 µM, LDN193189 5 µM, CHIR99021 15 µM, and DAPT 50 µM in a total volume of 100 µl were perfused through a mini-osmotic pump (Alzet, Cupertino, CA) for 7 days with a constant rate of 0.5 µl/hr. In control mice, 100 µl of 4% DMSO was perfused. Mice that received perfusion were sacrificed for immunostaining at 2 weeks post small molecule treatment.

### **Intraperitoneal injection of small molecules**

Core drug cocktail including CHIR99021, 2.79  $\mu\text{g}/10\text{g}$ ; DAPT, 8.65  $\mu\text{g}/10\text{g}$ ; LDN193189, 0.55  $\mu\text{g}/10\text{g}$ ; SB431542, 7.69  $\mu\text{g}/10\text{g}$  was injected into the peritoneum into 2-month old wildtype mice daily for 23 days. The vehicle solution (20% Captisol) was injected into WT mice (0.2ml/10g) as control. Starting from day 5, BrdU (0.1 ml/ 10 kg) was administrated every 3 to 4 days until day 26. At 32 days post the initial drug treatment, mice were sacrificed, perfused with artificial cerebral spinal fluid (ACSF). Brains were collected and post fixed in 4% paraformaldehyde. The fixed brains were washed with PBS and sectioned into 40  $\mu\text{m}$  slices. Brain slices were permeabilized and blocked with 0.3% Triton, 5% normal donkey serum and incubated with primary antibodies (Rabbit anti Ki67, Goat anti DCX) at 4°C overnight. The following day, brain slices were washed with PBS and incubated with secondary antibodies (Dylight 488 Donkey anti Rabbit and Dylight 647 Donkey anti Goat). After being washed with PBS, brain slices were mounted. Images were acquired using Zeiss LSM 800 confocal microscope. Scale bar: 20  $\mu\text{m}$ .

### **Supplemental References**

Kim, D., Landmead, B., and Salzberg, S.L. (2015). HISAT: a fast spliced aligner with low memory requirements. *Nat Methods* 12, 357-U121.

Pertea, M., Pertea, G.M., Antonescu, C.M., Chang, T.C., Mendell, J.T., and Salzberg, S.L. (2015). StringTie enables improved reconstruction of a transcriptome from RNA-seq reads. *Nat Biotechnol* 33, 290-+.